

NASA/TM-1998-206556



Forebody Flow Visualization on the F-18 HARV With Actuated Forebody Strakes

*David F. Fisher and Daniel G. Murri
Dryden Flight Research Center
Edwards, California*

National Aeronautics and
Space Administration

Dryden Flight Research Center
Edwards, California 93523-0273

September 1998

NOTICE

Use of trade names or names of manufacturers in this document does not constitute an official endorsement of such products or manufacturers, either expressed or implied, by the National Aeronautics and Space Administration.

Available from the following:

NASA Center for AeroSpace Information (CASI)
7121 Standard Drive
Hanover, MD 21076-1320
(301) 621-0390

National Technical Information Service (NTIS)
5285 Port Royal Road
Springfield, VA 22161-2171
(703) 487-4650

FOREBODY FLOW VISUALIZATION ON THE F-18 HARV WITH ACTUATED FOREBODY STRAKES

David F. Fisher¹ Daniel G. Murri²

Keywords: aircraft, F-18, flight, flight test, forebody, flow visualization, smoke, strake, vortical flow, vortex

Abstract

Off-surface smoke flow visualization and extensive pressure measurements were obtained on the forebody of the NASA F-18 High Alpha Research Vehicle equipped with actuated forebody strakes. Test points at $\alpha = 50^\circ$ were examined in which only one strake was deflected or in which both strakes were deflected differentially. The forebody pressures were integrated to obtain forebody yawing moments. Results showed that small single strake deflections can cause an undesirable yawing moment reversal. At $\alpha = 50^\circ$, this reversal was corrected by deploying both strakes at 20° initially, then differentially from 20° to create a yawing moment. The off-surface flow visualization showed that in the case of the small single strake deflection, the resulting forebody/strake vortex remained close to the surface and caused accelerated flow and increased suction pressures on the deflected side. When both strakes were deflected differentially, two forebody/strake vortices were present. The forebody/strake vortex from the larger deflection would lift from the surface while the other would remain close to the surface. The nearer forebody/strake vortex would cause greater flow acceleration, higher suction pressures and a yawing moment on that side of the forebody. Flow visualization provided a clear description of the strake vortices fluid mechanics.

Nomenclature

$C_{n0, fb}$	forebody (F.S. = 60 to 190) yawing moment at $\beta = 0^\circ$ from integrated pressures
C_p	pressure coefficient, $(p - p_0)/q_\infty$
F.S.	fuselage station, in.
HARV	High Alpha Research Vehicle
LEX	leading edge extensions
M	Mach number
p	local pressure, lb/ft ²
p_0	free-stream static pressure, lb/ft ²
q_∞	free-stream dynamic pressure, lb/ft ²
α	aircraft angle of attack, deg, (from left wingtip angle-of-attack vane corrected for upwash and boom bending)
β	aircraft angle of sideslip, deg, (average of left- and right-wingtip sideslip vanes corrected for angle of attack, deg)
$\delta_{s,d}$	differential strake deflection, right strake deflection minus left strake deflection, deg
$\delta_{s,L/R}$	left and right strake deflection measured from the retracted position, deg
θ	forebody cross-section circumferential angle, deg (0° is bottom centerline, positive is clockwise as seen from a front view, 0° to 360°)

Contact author: David F. Fisher,¹ Daniel F. Murri²

¹NASA Dryden Flight Research Center, Edwards, CA 93523-0273.

²NASA Langley Research Center, Hampton, VA 23681-001.

Introduction

The NASA High Angle-of-Attack Technology Program was initiated to increase understanding,

improve prediction techniques, provide design guidelines, and investigate new concepts for controls effectors on advanced, highly maneuverable aircraft at high angles of attack. The F-18 High Alpha Research Vehicle (HARV) at NASA Dryden Flight Research Center was a large part of that program. References 1, 2 and 3 described on-surface and off-surface flow visualization on the basic F-18 HARV configuration forebody and leading-edge extensions vortical flow fields at high angles of attack.[1, 2, 3] Recently, actuated forebody strakes were installed on the F-18 HARV radome and were designed to provide increased levels of yaw control at high angles of attack where conventional rudders become ineffective. This paper describes and reports flight results from off-surface flow visualization and forebody pressure distributions of the F-18 HARV with actuated forebody strakes at high angle of attack. Reference 4 provides additional details of these flight tests.[4]

Description

The F-18 HARV (fig. 1) is a highly instrumented F/A-18 aircraft that has been modified with thrust vectoring and actuated forebody strakes for maneuvering flight at high angles of attack.[5] Forty-eight-inch-long (122 cm) hydraulically operated forebody strakes were installed in the radome and positioned longitudinally 120° up from the bottom of the forebody, beginning 8 in. (20 cm) aft of the nose apex. The strakes are conformal with the forebody when retracted. A sketch of the strakes is shown in figure 2.

On certain flights, smoke flow visualization was used to mark and identify the off-surface behavior of the forebody/strike vortices. White smoke from a smoke generator system used previously on the F-18 HARV [1, 6] was fed from the smoke generator system through a single 1.5-in. diameter tube to the two 1.0-in. diameter ports located symmetrically 60° up on the nose cap. Figure 3 shows a closeup of the right smoke port and radome after a flight.

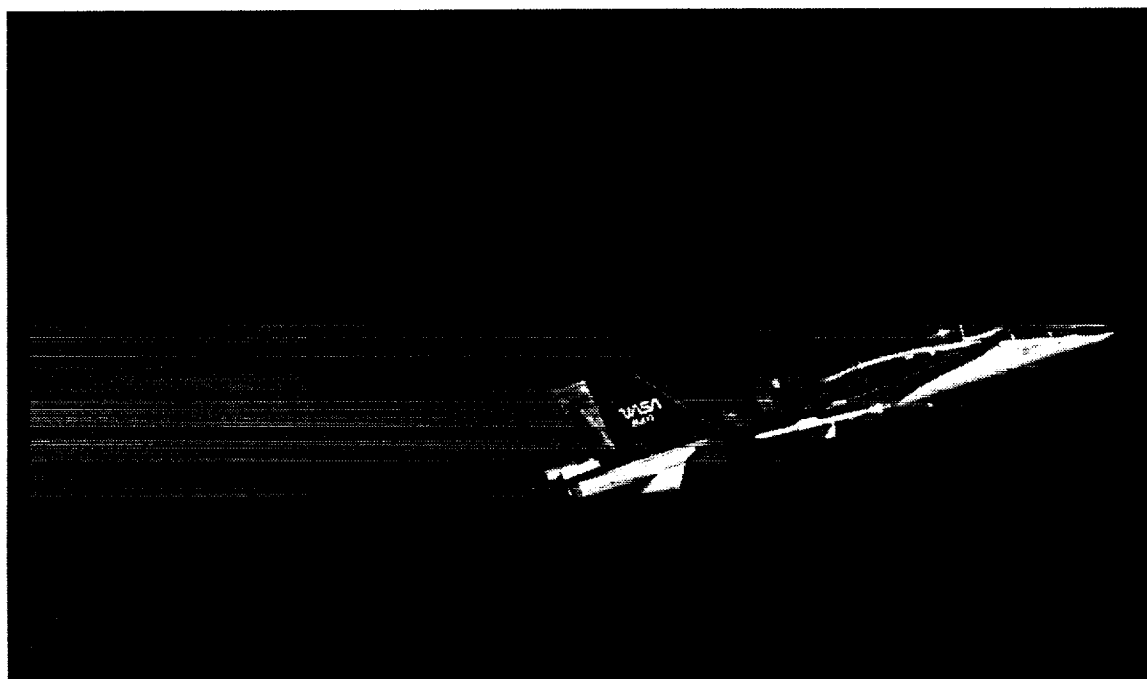


Figure 1. F-18 HARV aircraft with forebody strakes, $\alpha = 30^\circ$, δs , $L/R = 0^\circ/90^\circ$.

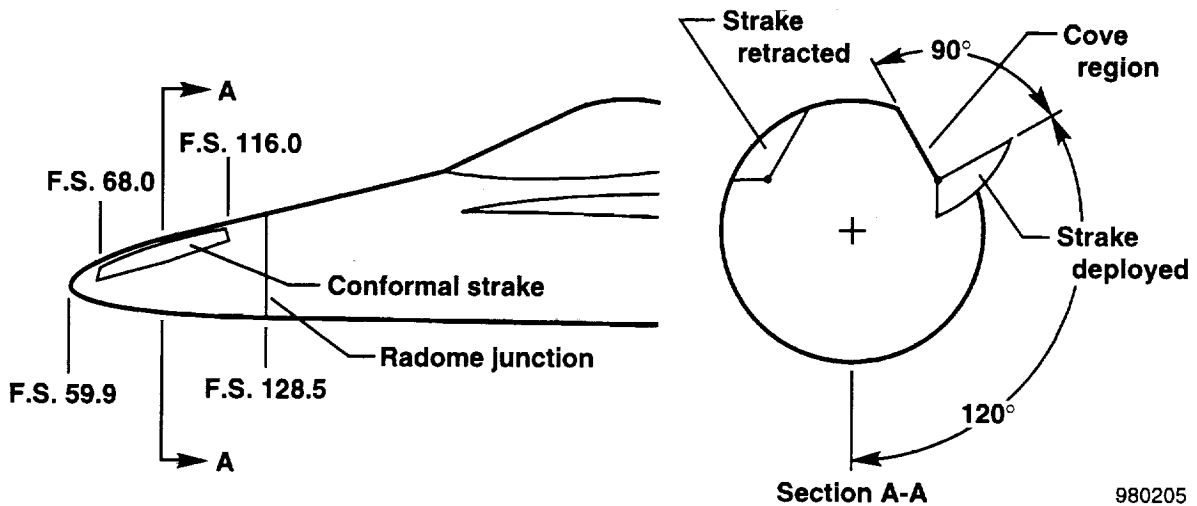


Figure 2. Sketch of forebody strakes on the F-18 HARV.

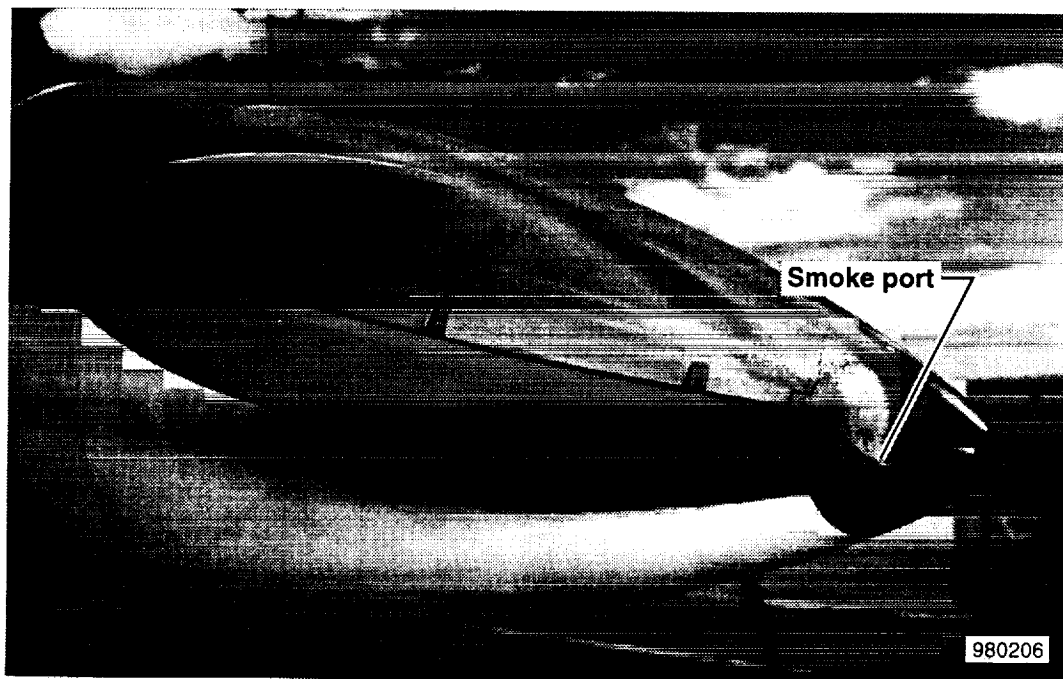


Figure 3. Close-up of right smoke port and strake on the F-18 HARV radome.

The fuselage forward of the cockpit was extensively instrumented with surface pressure measurements (fig. 4). Five circumferential rings of pressure orifices were installed on the surface of the radome, strakes, and forward fuselage, forward of the cockpit canopy at fuselage station (F.S.) 70, F.S. 85, F.S. 107, F.S. 142, and F.S. 184. More detailed information of the

instrumentation can be found in references 4 and 7.[4, 7]

Flight Test Conditions

Data presented in this paper were obtained from quasi-stabilized 1-g flight maneuvers at a nominal altitude of 25,000 ft and $M \approx 0.25$ for $\alpha \approx 50^\circ$. The pressure distribution data and the smoke

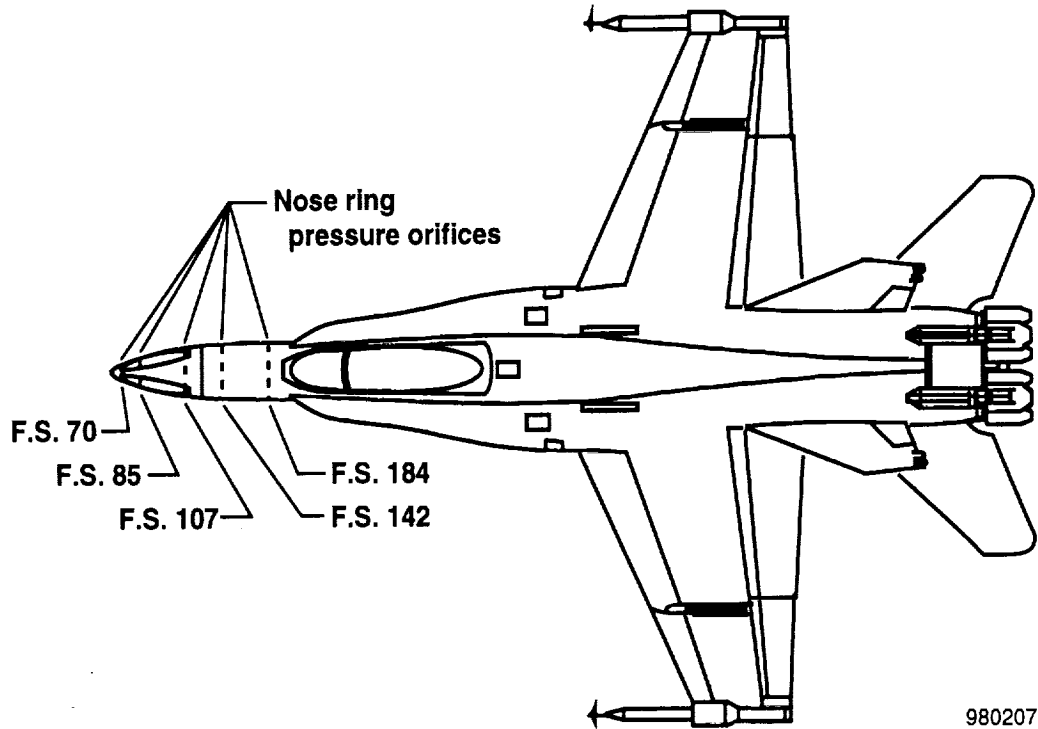


Figure 4. Location of pressure orifices on F-18 HARV forebody.

flow visualization data were obtained on separate flights because the smoke residue would cover some of the pressure orifices near the nose apex.

Results

During development in wind-tunnel tests [8], deflecting one strake at a time (fig 5(a)) at high angles of attack could result in a small but undesirable control reversal at small strake deflections. To overcome this undesirable characteristic for closed-loop control, a solution was developed that deploys both strakes symmetrically as angle of attack increases. Using the dual strake schedule (fig. 5(b)) at $\alpha = 50^\circ$ both strakes would be open initially at 20° . When a yawing moment is desired under these conditions, the strakes are deflected differentially about the 20° strake position as shown in figure 5(b). For example, with this strake schedule, a differential strake deflection of 30° , (right strake deflection minus left strake deflection), $\delta_{s,d} = 30^\circ$ would correspond to $\delta_{s,L/R} = 5^\circ/35^\circ$. For $\delta_{s,d} = 40^\circ$, the

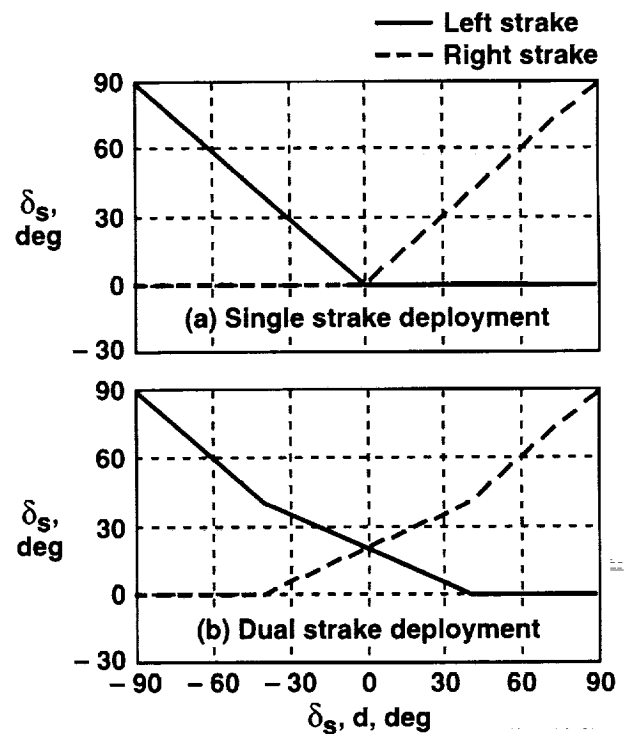


Figure 5. Strake deployment schedules.

left strake would be closed and the right strake would be open 40° . For increasing yawing moment, the right strake would continue to open, such that for all angles of attack, the maximum yaw control deflection would always consist of one strake fully deployed (90°) and the other strake fully retracted (0°).

Figure 6 shows the forebody yawing moments from flight as a function of differential strake deflection, $\delta_{s,d}$, at $\alpha = 50^\circ$. The forebody yawing moments were obtained by integrating the pressures measured on the forebody and strakes at the five forebody fuselage stations (fig. 4). Data for the single strake deployment show a large undesirable control reversal at $\delta_{s,d} < 30^\circ$. In this case, as the strakes begin to open, the yawing moment is opposite to the desired direction. The dual strake deployment eliminates the control reversal and results in a desirable, nearly linear, variation of forebody yawing moment for differential strake deflections.

Flow visualization of the forebody strake vortices were obtained by emitting smoke out of

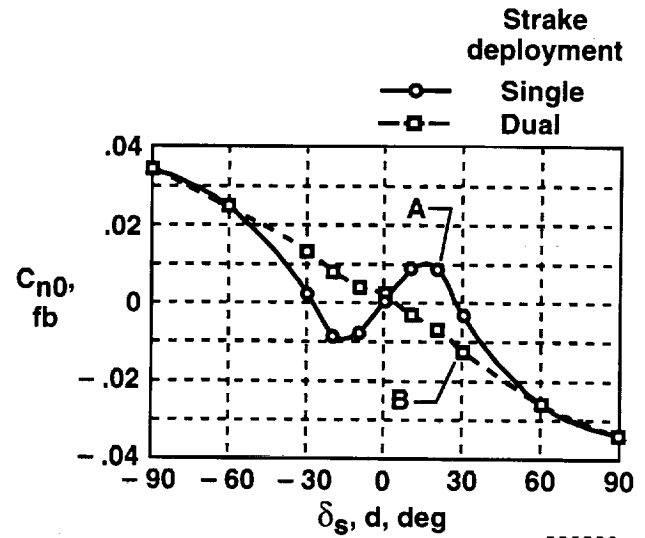


Figure 6. Forebody yawing moments as a function of differential strake position, $\alpha = 50^\circ$, $\beta = 0^\circ$.

the orifices at the nose apex and documenting the vortical flows with a still camera on the right wingtip and with video cameras on the left wingtip, heads-up display, and vertical tails. Figure 7 is a photo from the right wingtip of the

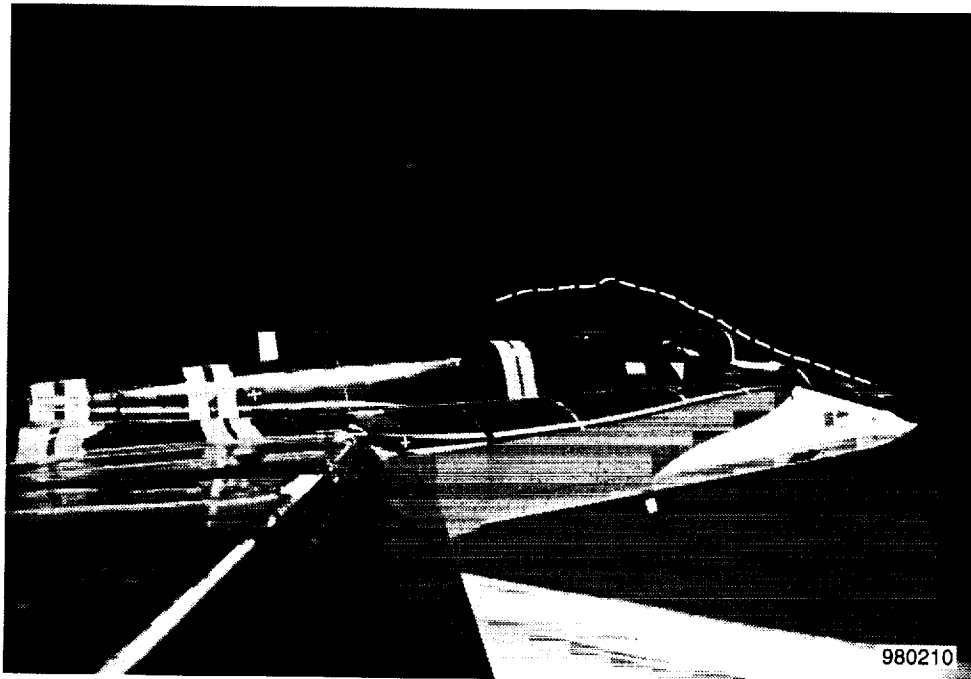


Fig. 7. Forebody/strake vortex flow visualization for $\alpha = 50^\circ$, $\delta_{s,d} \approx 19^\circ$, and $\delta_s, L/R = 0^\circ/19^\circ$.

forebody/strike vortices at $\alpha = 49.1^\circ$ and $\delta_{s, L/R} = 0^\circ/19^\circ$ (the left strike is retracted and the right strike is open 19°). This corresponds to point A on figure 6 near the occurrence of the maximum yawing moment reversal. At this point a yawing moment to the right occurs instead of the desired yawing moment to the left. In this photo (fig. 7), only the right vortex can be seen and it is low and close to the forebody surface. A dashed line is added to the figure to enhance the visibility of the vortex in the photo. The left vortex is apparently weaker and did not entrain any of the smoke.

The corresponding pressure distribution on the forebody at these conditions is shown in figure 8. This figure shows the forebody pressure distributions as a function of the forebody cross-section circumferential angle, θ , and includes a sketch of the vortical flow structure concept. Negative or suction pressure coefficients are plotted above $C_p = 0$ while positive pressure coefficients are plotted below $C_p = 0$. The vertical scales for each measurement station are offset by $C_p = 1$ from the previous measurement station.

The scale for the circumferential angle is reversed, so that the pressure distributions can be viewed from the pilot's perspective. The $\theta = 0^\circ$ and 360° are on the lower centerline; $\theta = 180^\circ$ is on the top centerline; $\theta = 90^\circ$ is on the right side of the fuselage; and $\theta = 270^\circ$ is on the left. This convention was established in previous papers. [4, 7] The cove region is the area on the fuselage exposed when the strike opens. Pressures were not available at F.S. 70 but were obtained at F.S. 85 and F.S. 107. The large suction peaks at $\theta \approx 160^\circ$ for F.S. 85 and F.S. 107 are caused by the right forebody/strike vortex. The right vortex footprints can also be seen at F.S. 142 and F.S. 184. At $\alpha = 50^\circ$, vortices naturally form on the forebody.[7] The left vortex suction peaks can be seen at F.S. 85, F.S. 107 and F.S. 142 at $\theta \approx 200^\circ$ and the smaller suction peaks suggest a weaker vortex than the right vortex. At F.S. 184, the right vortex has moved inboard and is centered over the forebody at $\theta = 180^\circ$, as marked by its suction footprint at that point, while the left

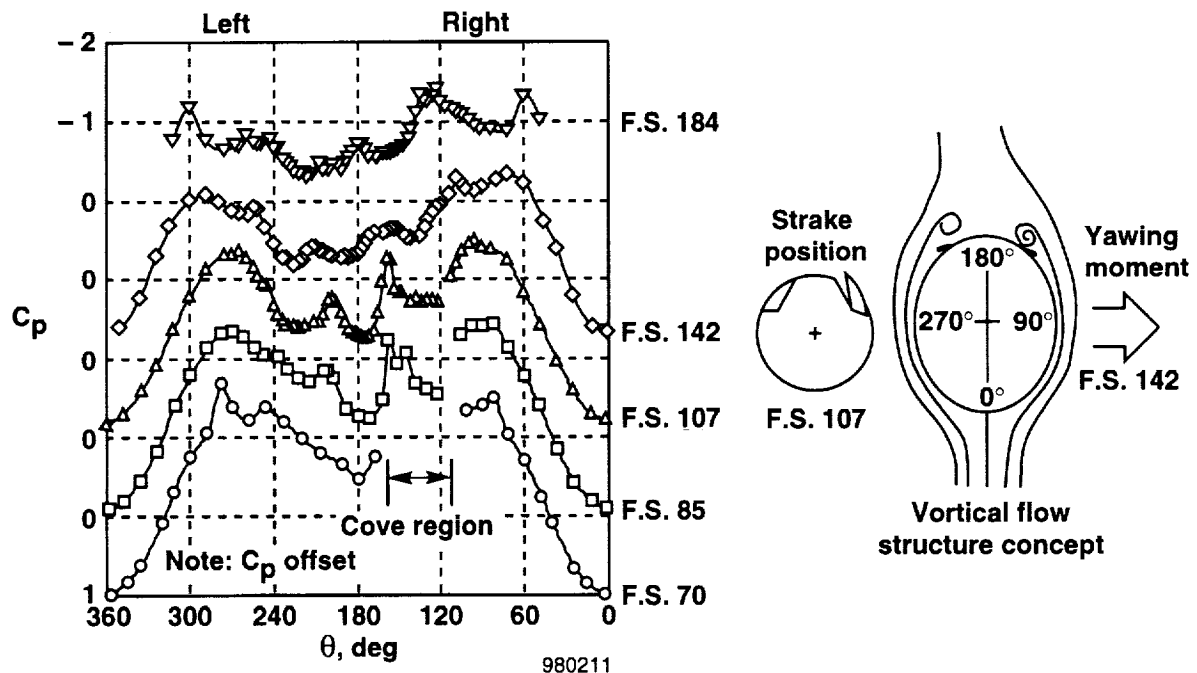


Figure 8. Forebody pressure distribution for $\alpha = 49.1^\circ$, $\beta = 2.1^\circ$, $\delta_{s,d} \approx 20^\circ$, and $\delta_{s, L/R} = 0^\circ/20^\circ$.

vortex has lifted from the surface, noted by the absence of a suction peak. With the right forebody/strike vortex close to the surface (see schematic), the flow on the right side is accelerated around the right side causing suction pressures that are higher than on the left side. Note the overall increased suction levels at $\theta = 60^\circ$ to 120° (right side) at F.S. 142 and 184 as compared with $\theta = 240^\circ$ to 300° (left side). The overall suction pressures are higher on the right side of the forebody than the left, hence, a yawing moment to the right.

Contrast the vortical flow shown previously in figure 8 with the vortical flow in figure 9 taken at $\alpha = 47.1^\circ$ and $\delta_{s, L/R} = 5^\circ/35^\circ$. In this case, both strakes opened initially to 20° , then, to create a yawing moment, the right strake opened 15° further to a deflection of 35° while the left strake closed 15° to a deflection of 5° . The differential strake deflection is (35° minus 5°) or 30° and this corresponds with point B on figure 6 with a yawing moment to the left, the desired direction.

In the figure 9 photo, two forebody/strike vortices are present. The right strake, which is deflected 35° , created a strong vortex that can be seen lifted from the surface, and although not shown here, remains coherent past the end of the aircraft. The left strake, deflected at 5° , created a weaker vortex that is low and close to the surface, eventually getting pulled down into the left LEX vortex.

Figure 10 shows the forebody pressure distributions corresponding to the dual strake deflections of $\delta_{s, L/R} = 5^\circ/35^\circ$ and vortex formations in figure 9. At F.S. 85, with the right strake open 35° , there is a large suction peak at $\theta \approx 160^\circ$ caused by the right forebody strake vortex. However, the suction peak diminishes moving aft to F.S. 107, then to F.S. 142, and is not present at all at F.S. 184. The suction peaks diminished because the right vortex had lifted from the surfaces, as shown in figure 9. At these conditions, the left forebody/strike vortex stayed close to the surface (as shown by the progressing

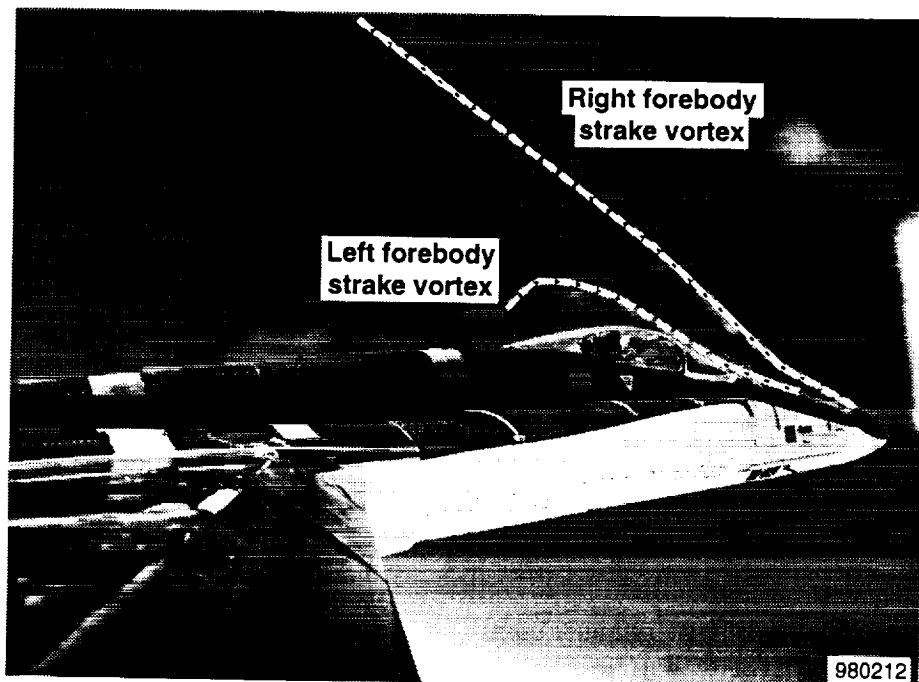


Figure 9. Forebody/strike vortex flow visualization for $\alpha = 50^\circ$, $\delta_{s, d} \approx 30^\circ$, and $\delta_{s, L/R} = 5^\circ/35^\circ$.

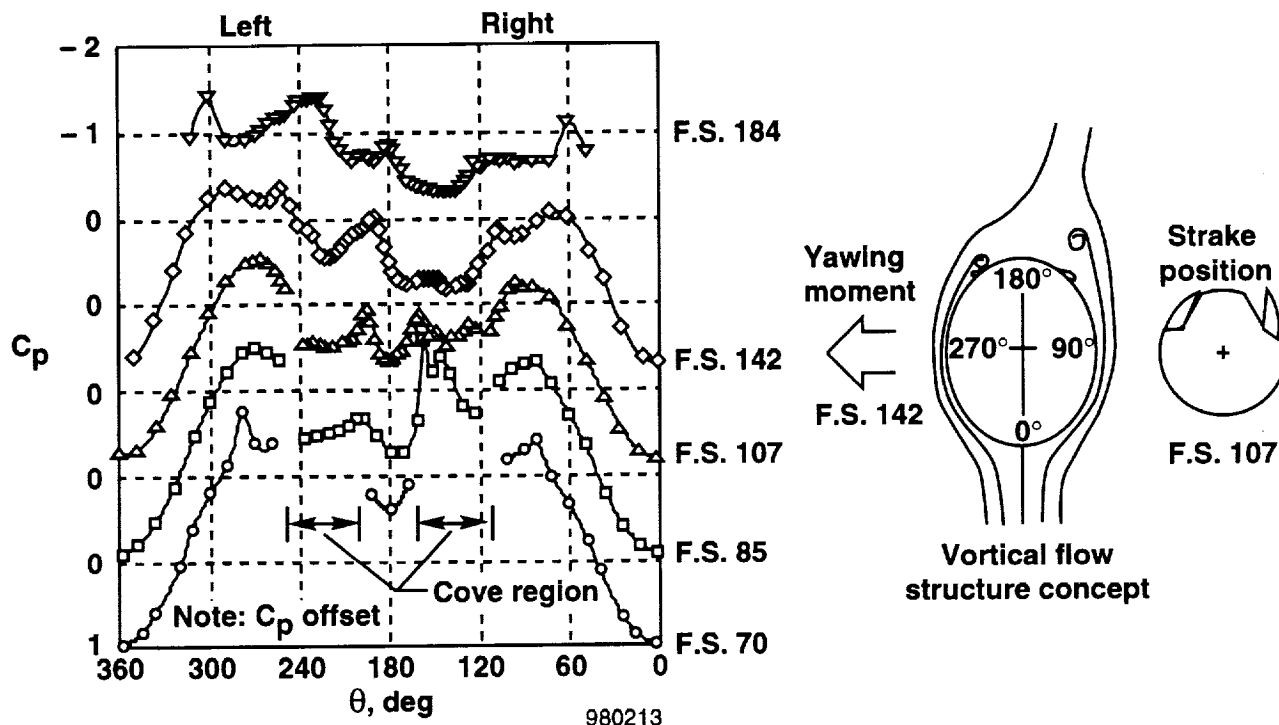


Figure 10. Forebody pressure distribution for $\alpha = 50^\circ$, $\delta_{s,d} \approx 30^\circ$, and $\delta_{s,L/R} = 5^\circ/35^\circ$.

increase in the suction peaks on the left side) reaching a maximum at F.S. 142. At F.S. 184, the left forebody/strake vortex is centered over the forebody at $\theta = 180^\circ$, as noted by the suction peak. The right forebody/strake vortex is farther from the surface and has less influence on the forebody pressures than the left forebody/strake vortex (which remained close to the surface). Consequently, the flow is accelerated around the left side creating higher suction pressures than on the right and resulting in a yawing moment to the left, as shown in the sketch (fig. 10).

Figure 11 shows the forebody vortex flow field at $\alpha \approx 47^\circ$ and $\delta_{s,L/R} = 0^\circ/90^\circ$, the left strake is closed and the right strake fully open. In this figure, both the left and right forebody vortices are clearly visible. The right vortex is lifted from the surface and remains coherent beyond the end of the aircraft while the left vortex remains close to the surface of the forebody and lifts at the canopy. The corresponding pressure distributions

are shown in figure 12 with a sketch of the vortical flow. There is a large right forebody/strake vortex footprint at F.S. 85, but it diminishes moving aft. The left forebody vortex footprints are clearly visible at F.S. 85 through F.S. 184. The right strake at 90° retarded the flow about the right side of the forebody. For example, at F.S. 107 (fig. 12), the maximum suction pressure coefficient on the right side at $\theta \approx 80^\circ$ was about $C_p \approx -0.6$. In figure 8, for $\delta_{s,L/R} = 0^\circ/20^\circ$, the maximum suction pressure coefficient at $\theta \approx 90^\circ$ was about $C_p \approx -1.5$. The left forebody vortex at $\delta_{s,L/R} = 0^\circ/90^\circ$ accelerated the flow about the left side and resulted in much higher suction pressures on the left side than on the right and a large yawing moment to the left.

For all three cases shown, flow visualization provided a clear description of the fluid mechanics of the strake vortices and their effect on the forebody forces.

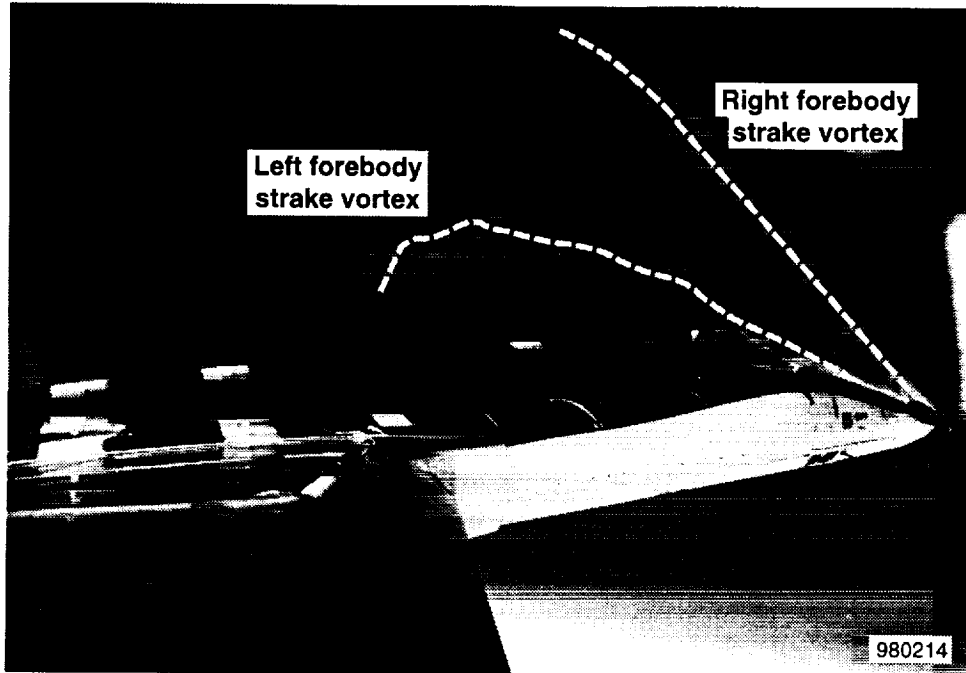


Figure 11. Forebody/strike vortex flow visualization for $\alpha = 47.2^\circ$, $\beta = 3.9^\circ$ and $\delta_s, L/R = 0^\circ/90^\circ$.

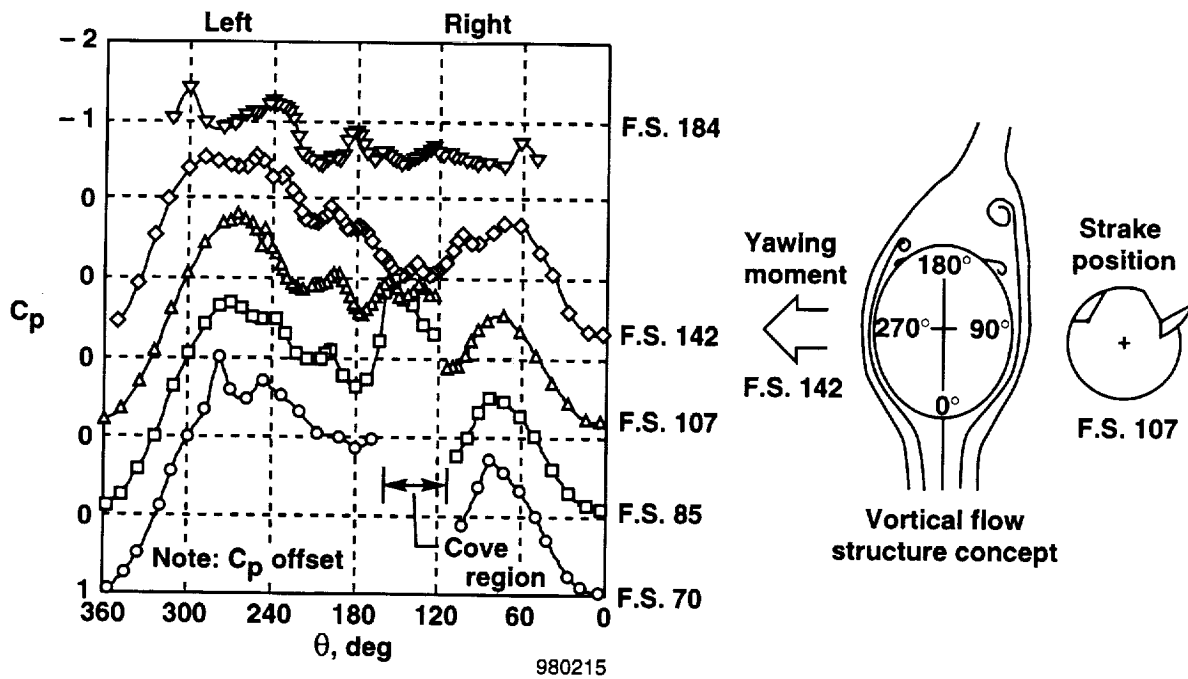


Figure 12. Forebody pressure distribution for $\alpha = 50^\circ$, $\delta_s, d \approx 90^\circ$, and $\delta_s, L/R = 0^\circ/90^\circ$.

Concluding Remarks

Off-surface smoke flow visualization and extensive pressure measurements were obtained on the forebody of the NASA F-18 High Alpha Research Vehicle equipped with actuated forebody strakes. Test points at $\alpha = 50^\circ$ were examined, in which only one strake was deflected or in which both strakes were deflected differentially. The forebody pressures were integrated to obtain forebody yawing moments, and showed that small single strake deflections can cause an undesirable yawing moment reversal. At $\alpha = 50^\circ$, this reversal was corrected by deploying both strakes initially at 20° , then differentially from that point to create a yawing moment. The off-surface flow visualization showed that in the case of the small single strake deflection, the resulting forebody/strake vortex remained close to the surface and caused accelerated flow and higher suction pressures on that side. When both strakes were deflected differentially, two forebody/strake vortices were present. The forebody/strake vortex with the larger deflection would lift from the surface while the other would remain close to the surface. The nearer forebody/strake vortex would cause greater flow acceleration, increased suction pressures and a yawing moment on that side of the forebody. Flow visualization provided a clear description of the strake vortices fluid mechanics.

References

- [1] Fisher, D. F., Curry, R. E., Del Frate, J. H., and Richwine, D. M.; "In-flight flow visualization techniques on a vortex-lift fighter aircraft," FLOW VISUALIZATION V, Proceedings of the Fifth International Symposium on Flow Visualization, Prague, Czechoslovakia, August 21-25, 1989, pp. 543-548.
- [2] Del Frate, John H. and Zuniga, Fanny A.; "In-flight flow field analysis on the NASA F-18 High Alpha Research Vehicle with comparisons to ground facility data." *Proceedings of the 28th Aerospace Sciences Meeting*, Reno, Nevada, AIAA-90-0231, January 1990.
- [3] Fisher, David F., Del Frate, John H., and Richwine, David M.; *In-Flight Flow Visualization Characteristics of the NASA F-18 High Alpha Research Vehicle at High Angles of Attack*. NASA TM-4193, May 1990.
- [4] Fisher, David F., Murri, Daniel G. and Lanser, Wendy R.; *Effect of actuated forebody strakes on the forebody aerodynamics of the NASA F-18 HARV*. NASA TM-4774, October 1996.
- [5] Bowers, Albion H., Pahle, Joseph W., Wilson, R. Joseph, Flick, Bradley C., and Rood, Richard L.; *An overview of the NASA F-18 High Alpha Research Vehicle*. NASA-TM-4772, October 1996.
- [6] Curry, Robert E. and Richwine, David M.; "An airborne system for vortex flow visualization on the F-18 High-Alpha Research Vehicle." *AIAA/NASA/AFWAL Sensors and Measurements Technology Conference*, Atlanta, Georgia, AIAA-88-4671, September 7-9, 1988.
- [7] Fisher, David F., Banks, Daniel W., and Richwine, David M.; *F-18 High Alpha Research vehicle surface pressures: initial in-flight results and correlation with flow visualization and wind-tunnel data*. NASA TM-101724, August 1990.
- [8] Murri, Daniel G., Shah, Gautam H., DiCarlo, Daniel J., and Trilling, Todd W.; "Actuated forebody strake controls for the F-18 High-Alpha Research Vehicle." *J. of Aircraft*, vol. 32, no. 3, pp. 555-562, 1995.

REPORT DOCUMENTATION PAGE			Form Approved OMB No. 0704-0188	
Public reporting burden for this collection of information is estimated to average 1 hour per response, including the time for reviewing instructions, searching existing data sources, gathering and maintaining the data needed, and completing and reviewing the collection of information. Send comments regarding this burden estimate or any other aspect of this collection of information, including suggestions for reducing this burden, to Washington Headquarters Services, Directorate for Information Operations and Reports, 1215 Jefferson Davis Highway, Suite 1204, Arlington, VA 22202-4302, and to the Office of Management and Budget, Paperwork Reduction Project (0704-0188), Washington, DC 20503.				
1. AGENCY USE ONLY (Leave blank)		2. REPORT DATE September 1998		3. REPORT TYPE AND DATES COVERED Technical Memorandum
4. TITLE AND SUBTITLE Forebody Flow Visualization on the F-18 HARV With Actuated Forebody Strakes			5. FUNDING NUMBERS WU 529-31-04-00-37-00-F18	
6. AUTHOR(S) David F. Fisher and Daniel G. Murri				
7. PERFORMING ORGANIZATION NAME(S) AND ADDRESS(ES) NASA Dryden Flight Research Center P.O. Box 273 Edwards, California 93523-0273			8. PERFORMING ORGANIZATION REPORT NUMBER H-2254	
9. SPONSORING/MONITORING AGENCY NAME(S) AND ADDRESS(ES) National Aeronautics and Space Administration Washington, DC 20546-0001			10. SPONSORING/MONITORING AGENCY REPORT NUMBER NASA/TM-1998-206556	
11. SUPPLEMENTARY NOTES Presented at the 8th International Symposium on Flow Visualization, Sorrento, Italy Sept. 1-4, 1998.				
12a. DISTRIBUTION/AVAILABILITY STATEMENT Unclassified—Unlimited Subject Category 02			12b. DISTRIBUTION CODE	
13. ABSTRACT (Maximum 200 words) Off-surface smoke flow visualization and extensive pressure measurements were obtained on the forebody of the NASA F-18 High Alpha Research Vehicle equipped with actuated forebody strakes. Test points at $\alpha = 50^\circ$ were examined in which only one strake was deflected or in which both strakes were deflected differentially. The forebody pressures were integrated to obtain forebody yawing moments. Results showed that small single strake deflections can cause an undesirable yawing moment reversal. At $\alpha = 50^\circ$, this reversal was corrected by deploying both strakes at 20° initially, then differentially from 20° to create a yawing moment. The off-surface flow visualization showed that in the case of the small single strake deflection, the resulting forebody/strake vortex remained close to the surface and caused accelerated flow and increased suction pressures on the deflected side. When both strakes were deflected differentially, two forebody/strake vortices were present. The forebody/strake vortex from the larger deflection would lift from the surface while the other would remain close to the surface. The nearer forebody/strake vortex would cause greater flow acceleration, higher suction pressures and a yawing moment on that side of the forebody. Flow visualization provided a clear description of the strake vortices fluid mechanics.				
14. SUBJECT TERMS Aircraft, F-18, Flight, Flight Test, Flow visualization, Forebody, Smoke, Strake, Vortex, Vortical flow			15. NUMBER OF PAGES 16	
			16. PRICE CODE A03	
17. SECURITY CLASSIFICATION OF REPORT Unclassified	18. SECURITY CLASSIFICATION OF THIS PAGE Unclassified	19. SECURITY CLASSIFICATION OF ABSTRACT Unclassified	20. LIMITATION OF ABSTRACT Unlimited	

